ISSN 0018-1439, High Energy Chemistry, 2022, Vol. 56, No. 2, pp. 73–90. © Pleiades Publishing, Ltd., 2022.

REVIEW

Environment Friendly g-C_3N_4-Based Catalysts and Their Recent Strategy in Organic Transformations

Murugan Arunachalapandi[a] and Selvaraj Mohana Roopan[a, *]

[a] *Chemistry of Heterocycles and Natural Products Lab, Department of Chemistry, School of Advanced Sciences, Vellore Institute of Technology, Vellore-632014, Tamilnadu, India*

**e-mail: mohanaroopan.s@vit.ac.in*

Received November 1, 2021; revised November 1, 2021; accepted November 3, 2021

Abstract—Organic molecules synthesized in an environmentally friendly manner have excellent therapeutic potential. The entire preparation technique was examined in the existence of a light source, implying that light has been replaced by heating and the usage of dangerous chemicals has decreased, resulting in less pollution of the environment. The advantages of these nanocarbon catalysts include high efficiency, environmentally friendly synthesis, eco-friendly, inexpensive, and non-corrodible. In organic transformations, solid metal base/metal-free catalysts produce better results. Here, the metal-free semiconductor g-C_3N_4 was used to demonstrate the catalytic behavior of organic conversions. g-C_3N_4 is a two-dimensional material and a p-type semiconductor to enhance the photocatalytic activity. The excellent properties of g-C_3N_4 sheet lead to the support of metals to form metal-organic frameworks. Most of the reactions gained positive response under visible light irradiation. This review will inspire readers in widen the applications of g-C_3N_4 based catalyst in various organic transformation reactions.

Keywords: heterogeneous catalysis, g-C_3N_4, nanosheets, organic reaction

DOI: 10.1134/S0018143922020102

1. INTRODUCTION

In the medical industry, every hour spent synthesizing a new chemical molecule is employed to treat ailments. Furthermore, the creation of new compounds produces toxic waste, which has negative consequences for our planet. Greener measures are employed to combat waste creation. Green synthesis is a type of synthesis that is both ecologically friendly and efficient. In this method, renewable raw materials and safer solvents were used. Also, this method ensures the avoidance of chemical accidents by preventing the hazardous substance production [1]. Having 12 principles of green chemistry in hand, we can rectify all the drawbacks in the preparation of organic compounds in the laboratory. The preparation needs some hazardous chemicals, heating equipment and conditions to get the final product. These conditions produce harmful effects on nature. Scientists have worked more to reduce these effects for the preparation of compounds [2]. So, they introduced green methods for the preparation of organic compounds such as catalysis and photocatalysis.

In the field of chemistry, catalysts play a vital role in enhancing the rate of reactions. Catalytic functions are essential for almost 90% of industrial processes [3]. All the times, many scientists were interested in developing chemical processes *via* catalytic approach. Such catalytic processes proceed through either homogeneous or heterogeneous medium. Homogeneous means the same phase and heterogeneous means the different phase of the reactants with respect to catalyst [4, 5]. Homogeneous catalysis has the advantage of high chemo-regio selectivity and high activity, but simultaneously, it has disadvantages such as reusability. The homogeneous reaction conditions were difficult to conduct at the laboratory level. To overcome the above-mentioned drawback, heterogeneous catalysts were used because they have merits such as catalyst recovery, excellent stability and easy accessibility. Also, heterogeneous catalysis has some demerits in the catalytic performance such that it takes more time to make contact with the catalyst and reactants [6]. Hence, researchers needed to develop a new combined system in catalysis. This new system has dynamics like homogeneous catalysts and effectively recoverable like heterogeneous catalysts [7].

Graphitic carbon nitride (g-C_3N_4) is a metal-free semiconductor that has a bandgap of 2.7 eV. g-C_3N_4 has high thermal stability and chemical properties suitable for work on organic reactions, degradation and water splitting. In 2009, g-C_3N_4 using photocatalysis was reported for hydrogen production [8]. g-C_3N_4

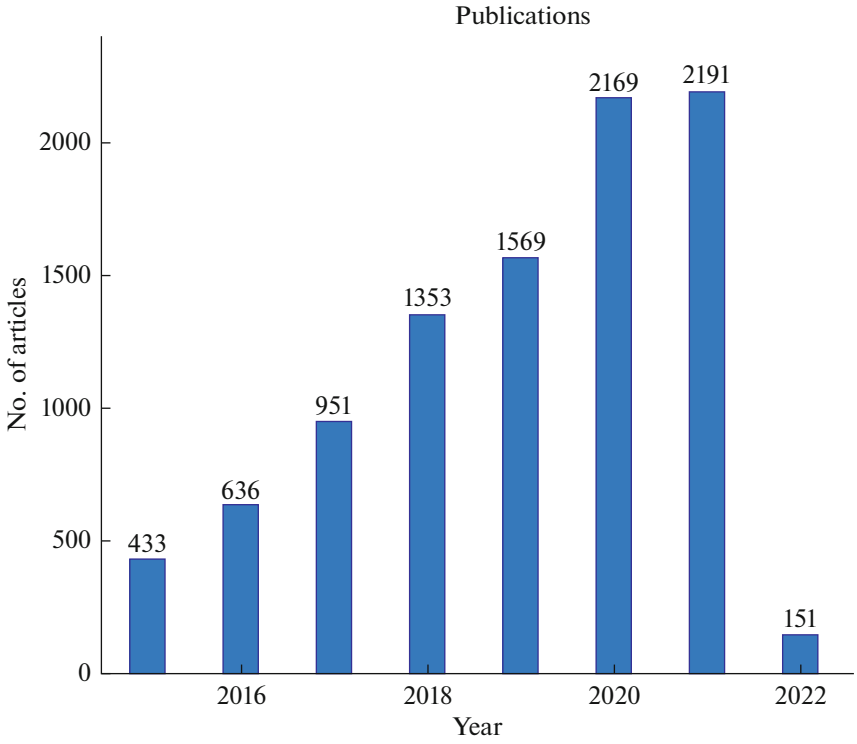

Fig. 1. List of publications in g-C_3N_4 based on Scopus data on 31 October 2021.

catalyst was used to significantly improve the catalytic behavior in increasing hydrogen production [9, 10]. g-C_3N_4 is a two-dimensional material and a *p*-type semiconductor to enhance the photocatalytic activity [11]. Many advanced synthetic methodologies were used to characterize g-C_3N_4 which led to the study of its activity in the reaction medium [12]. The catalytic properties of g-C_3N_4 have been improved by introducing metallic and nonmetallic elements such as boron and sulfur onto its surface [13]. Synthesis of g-C_3N_4 has been performed by co-polymerization of monomer with thermal condensation of nitrogen-rich forerunners such as thiourea [14, 15], dicyandiamide, melamine [16, 17], etc. g-C_3N_4 can be prepared from melamine monomer by the hydrothermal method to evaporate ammonia [18–21]. These already exist in many reviews highlighting the photocatalytic activity of g-C_3N_4 but only a few reviews focusing on g-C_3N_4 in catalyzing organic transformation reactions are reported. This review aims to explore various works regarding g-C_3N_4 to perform organic transformations in presence of visible light.

Vividly increasing attention is paid to g-C_3N_4 based photo-catalysts due to their exclusive electronic band structure and physicochemical properties. To improve the photocatalytic properties of g-C_3N_4, binding with any metal or doping with composite has to be done [22]. Such improved catalyst will be helpful in organic reactions. Generally, (organic reactions having reactive intermediates *via* activation energy to form the final products) the photogeneration of these reactive intermediates is mainly focused on organic synthesis [23–28]. However, the creation of these active species under mild reaction conditions and obeying the twelve principles of green chemistry is not an easy task [29, 30]. It was a green synthesized method because the light energy was directly used for the chemical reaction to occur [31]. In recent decades, researchers are interested in working on metal doped g-C_3N_4 polymer sheets to enhance the catalytic activity. Figure 1 shows the recent publications in g-C_3N_4, thus confirming it as an emerging catalyst in the field of catalysis. Pristine g-C_3N_4 has few restrictions because of its inadequate solar light absorption, decreased surface area and fast recombination of photo-generated electron hole-pairs in the field of photocatalysis [32–34]. Photons present in light deliver high energy into the molecules to form radicals. These radicals are recombined to give the products and no waste is generated in this process [35]. Applications in photochemical technique are that the reactants should get stabilized by the proton and go to the next singlet or triplet state via multiplicity of reactants. The above approach is applied to carbon inter-

mediate species having wide applications in organic synthesis [36–38].

g-C_3N_4 is a graphitic nanosheet having tunable properties with various applications such as easy synthesis [39], H_2 production from water [40], dye degradation [41], CO_2 exchanges [42] and organic synthesis. Two-dimensional structure functionalize the graphitic nature of g-C_3N_4 to reduce the band gap and slow the recombination of electrons at the valence band. The excellent properties of g-C_3N_4 sheet leads to support metals to form metal-organic frameworks [43–47]. If any heteroatom is doped in g-C_3N_4, it enhances the activity towards degradation applications. Nonmetallic elements such as sulfur, carbon, phosphorus, boron, fluorine, and iodine can also be bound with g-C_3N_4 to increase the light absorption and electron-hole recombination [48–51].

Heterocycles have core structures in biologically active compounds. Recently, plentiful efforts to engineer new organic molecules. New methods to prepare the heterocycles have been developed [52–58]. In recent decades, the synthesis of organic compounds in visible light has been difficult because of the photocatalyst deficit. It spoils the catalytic pathway of the reaction; hence, it need an upgrade to conduct the photo catalytic organic reaction. It tainted the activated catalytic system and then it became the most appropriate in the field of photocatalysis [59–66]. Photocatalysis in organic synthesis is more important because of its properties of redox transformation [67–70]. Inorganic semiconductors (TiO_2) are either UV or visible light active photocatalysts which are widely used to study the photocatalytic activity in hydrogen production from water [71]. Organic semiconductors are not given any special application because they vary in synthetic modularity thus changing their electronic and structural properties [72–74].

In 2019 Antonietti discussed g-C_3N_4 photocatalysis in a short review. Here they explain the activity of g-C_3N_4 in catalysis *via* organic transformations. In the same year Savateev exposed the current scenario of g-C_3N_4 catalyst and its applications in C–C bond forming reactions, dye degradation, and its semiconductor activities in catalysis field. In 2020, Luque reported a review of g-C_3N_4 catalyzed organic transformations [75–77].

All of the above reviews emphasized information on g-C_3N_4 catalyzed organic transformation, dye degradation, and semiconductor properties. In this review, the readers could able to understand current scenario on eco-friendly g-C_3N_4 based catalyst for organic reactions in the presence of light medium. The discussed schemes are effective in producing high yield products and reusability of the catalyst ensured the heterogeneity of g-C_3N_4.

2. APPLICATIONS OF g-C_3N_4

2.1. Oxidation

Recently, Lopez et al. reported the potassium containing C_3N_4 catalyst for the selective oxidation of 5-hydroxymethyl-2-furfural **1** to 2,5-furandicarboxaldehyde **2** [78]. **Scheme 1** shows K-C_3N_4 catalyzed selective oxidation of **1** and selectively conversion to **2** in 30 min with water and natural solar light was used directly as the source. The authors prepared three K-C_3N_4 catalysts using two ambient preparative methodologies involving no hazardous chemicals. Metal-free catalysts have a dominant approach in catalyzing nonmetallic reactions. Xin et al. expressed the photocatalytic activity of g-C_3N_4 in **Scheme 2.** Here, toluene was used and metal-free catalyst enhanced the oxidation of primary C–H bond to give **4** [79]. Toluene an active methylene group and it was converted into aldehyde form **3** in the presence of O_2. Preparation of g-C_3N_4 having a mesoporous structure was reported and it involved the straight oxidation of **3**. In the absence of a catalyst, auto-oxidation occurred to form byproducts of acids and esters. The mechanism of these reactions showed heterogeneous oxidation of toluene to form superoxide radicals on the mesoporous surface. The superoxide radical anion plays a key role in the oxidation of alcohols. The sheets of g-C_3N_4 were examined for 21 trails to check the selectivity to produce greater yield of **4**.

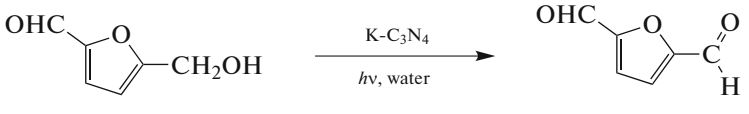

1 **2**

Scheme 1. Oxidation of 5-hydroxymethyl-2-furfural.

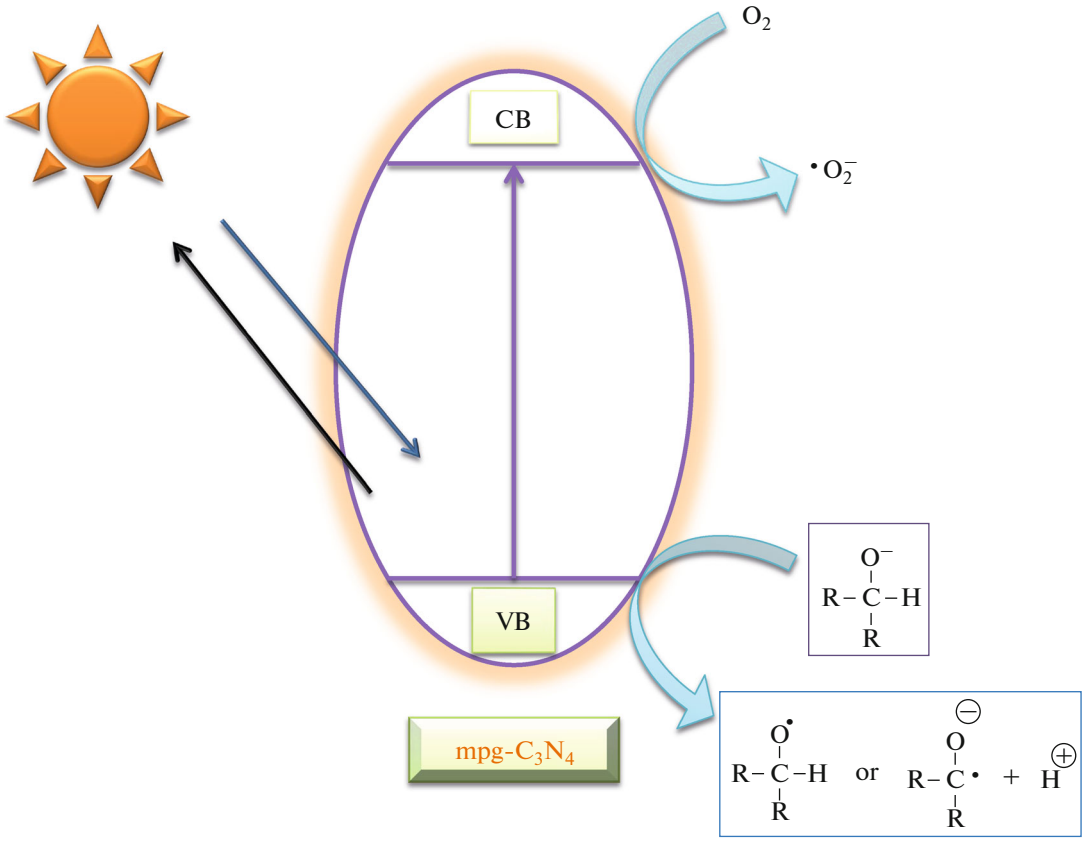

Fig. 2. Schematic explanation of Oxidation of alcohols.

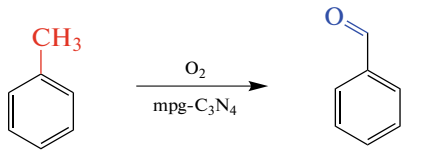

3 **4**

4 examples
99%

Scheme 2. Oxidation of primary C−H.

Fangzheng et al. published Scheme 3 in 2010, in which the g-C_3N_4 polymer functions as a catalyst to produce **6** from the oxidation of **5** [80, 81]. This was the first report in the 21st century to synthesize mpg-C_3N_4. Mpg-C_3N_4 had good catalytic activity in the selective alcohols to generate aldehydes. Mpg-C_3N_4 catalyst was nontoxic, metal-free, economic, and easy to recover from the reaction mixture. Previously, nitroxyl radicals were used to convert aldehydes, which are much more harmful, but here, moderate experimental conditions are used to create benzaldehydes. Metal-free heterogeneous catalysis was used in this selective oxidation to generate higher yields of **6**. The mechanism of Scheme 3 is shown in Fig. 2. Here light energy is used in mpg-C_3N_4 semiconductor to generate **6.** Scheme 4 shows the oxidation of the C-H bond which was activated with O_2 to form **7** in the presence of g-C_3N_4 catalyst. g-C_3N_4 is best metal-free catalyst for activating oxygen at high pressure. The 20% of graphene and carbon nitride showed good activity to produce a maximum yield of **8a** and a minor yield of **8b**. The cyclohexane compound has only sec-

ondary C-H bonds of saturated alkanes, which react with oxygen gas to form ketones. g-C_3N_4 was an organic semiconductor that was is more active in the presence of O_2 to produce radicals for this selective oxidation [82]. Also, the polymeric catalyst has high stability and chemoselectivity to activate the C-H bonds in **7** to give good yields.

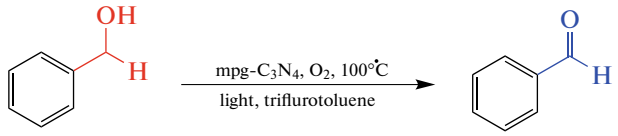

5 **6**
8 examples
90–99%

Scheme 3. Selective oxidation of alcohols.

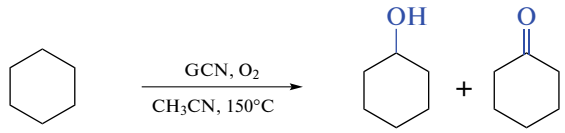

7 **8a** **8a**

8 examples
61–99 %

Scheme 4. Selective oxidation of secondary C–H.

The photocatalyzed selective oxidation of benzyl alcohol to benzaldehyde is a simple organic reaction that occurs in visible light. Verma et al. have already reported the same aldol condensation reaction between alcohols and corresponding ketones/aldehydes with the presence of mesoporous g-C_3N_4 and di-oxygen in 2010. Several catalysts were examined for a green method. Verma et al reported Scheme 5 another visible light active VO@g-C_3N_4 system, which was used for the selective oxidation of **9** [83]. The main advantage of g-C_3N_4 is use of renewable energy like sunlight and wind. Energy consumption around the globe is gradually increasing and several environmental problems are caused by the burning of fossil fuels. These drawbacks can be overcome by the utilization of renewable energy sources. Here, in the first step VO@g-C_3N_4 absorbs light and gets the energy to activate superoxide radicals on the surface. Superoxide radicals are active and react with alcohol/diols to generate the corresponding carbonyl compounds. The activity of VO@g-C_3N_4 was checked for 13 samples to give more than 90% yield of **10** under visible light.

Photocatalysis can be categorized into two groups; one is semiconductors (metal nanoparticles) and the other are metal complexes more active in UV light compared to visible light to conduct the photocatalytic process efficiently. Now semiconductor type metal-free carbon nanosheets are more active in a visible light region. Scheme 6 [84] explains the best semiconductor type catalyst for the removal of hydrogen atoms in **11** to form aromatic **12** and this was achieved with MnO_2@g-C_3N_4 in visible light. The secondary oxidizing agents (hydroxy radicals) directly react with **12** to form the product in the presence of light. 93% of products were obtained and recyclability of the catalyst was checked for several runs.

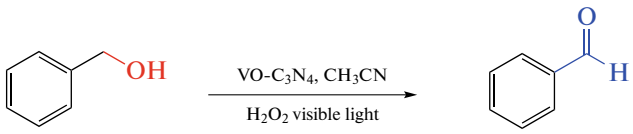

9 **10**
13 examples
95–98%

Scheme 5. Selective oxidation of alcohols.

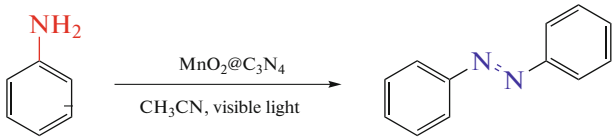

11 **12**
5 examples,
90–93%

Scheme 6. Oxidation of aromatic anilines.

Starting with a liquid precursor and creating the material using condensation technique, controlled porosity at the nanometric scale in the bulk of carbon nitride must improve its functionality. Scheme 7 describes the oxidation of **13** to produce **14** with noble metal-free catalyst g-C_3N_4. The reaction proceeds *via* the green route and O_2 acts as an oxidizing agent. Metal-free g-C_3N_4 is an excellent catalyst in visible light to give high yields of products. The high selectivity of g-C_3N_4 directs the esterification of **13** to form alcohol [85].

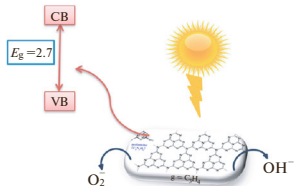

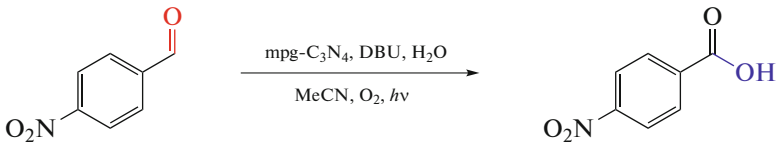

13 **14**

20 examples,
70–96%

Scheme 7. Selective oxidation of aldehydes.

Another example of the oxidation type of amidation process has been described by Wang et al. where Ag was anchored to g-C_3N_4 *via* condensation method [86]. The catalysts in an amidation reaction render the hydroxyl group free for activation before progressing to interact with an amine. The use of THF in place of amine led to the corresponding formation of an aldehyde. Most of the organic compounds are not active in the visible light region. Therefore, an external photocatalytic material is required for the organic transformation. Scheme 8 explains that Ag supported g-C_3N_4 exhibits excellent photocatalytic activity through the aerobic oxidative amidation of 1**5a** and **15b** under visible light irradiation. A 25W compact fluorescent light bulb was used for this reaction at room temperature. The reactions were green and mild reaction conditions to produce maximum yield of **16**.

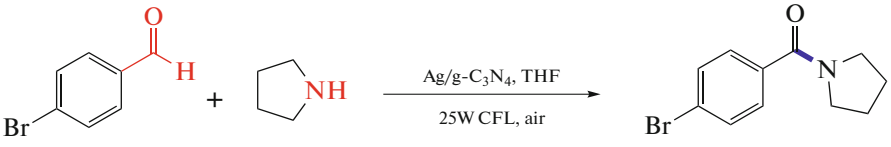

15a **15b** **16**

26 examples,
60–93%

Scheme 8. Oxidative amidation of aromatic aldehydes.

In 2017, Xu et al. worked on the catalysis study of CoPz supported g-C_3N_4 for the oxidation of 5-hydroxymethylfurfural [87]. Scheme 9 g-C_3N_4 was used to support the immobilized CoPz to generate a new hybrid catalyst for the selective oxidation of 5-hydroxymethylfurfural **17** into 2,5-furandicarboxylic acid. After 5 recycles, this catalyst showed good activity for performing the reaction.

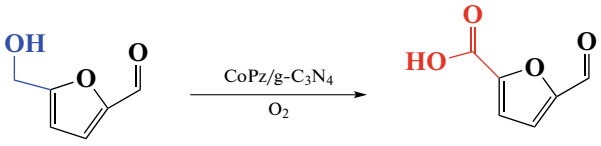

17 **18**

96%

Scheme 9. Oxidation of 5-hydroxymethylfurfural.

Polyacrylonitrile (PAN) supported on silver nanoparticles and g-C_3N_4 was fabricated by electrospinning method by Shah et al (88) in 2020. In Scheme 10 spherical silver nanoparticles placed with g-C_3N_4 material were dispersed in PAN surface without agglomeration. **19a–c** was converted into corresponding **20a** in the presence of visible light. The light active mediated reaction was initiated on the surface of g-C_3N_4, because of its photoactive nature. The properties of the catalyst were mesoporous, enhanced activity, and reusability. Ag supported catalyst was developed with selective oxidation to give epoxide (99%). C–H activation reaction was also carried out by the same catalyst to give 99% of yields. Scheme 11 was the first report on the sulfide oxidation of **21** to give **22** in the presence of winkler g-C_3N_4 and $^{\bullet}O_2^-$ and $^1O_2$ catalysts. the wrinkled C_3N_4 nanosheets cause an effi-

cient electron photoexcitation even in the presence of strong excitonic effects was confirmed in photoluminescence spectroscopy (89). The catalyst and cocatalyst show high selectivity towards sulfide oxidation.

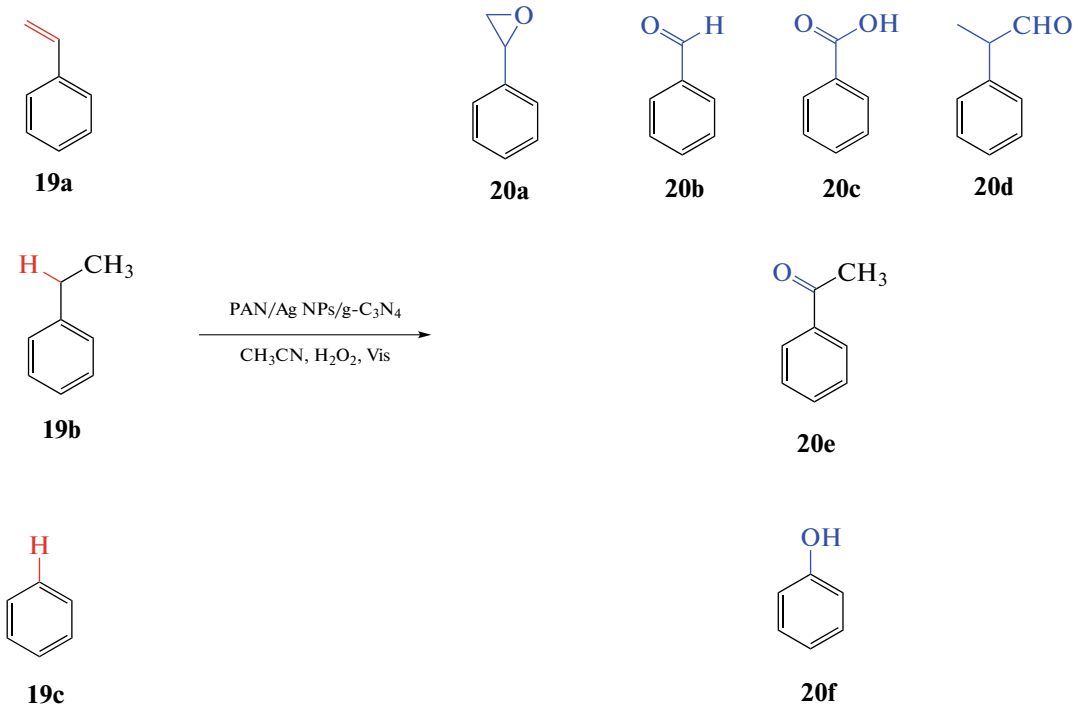

Scheme 10. Oxidation by PAN/AgNPs/g-C_3N_4.

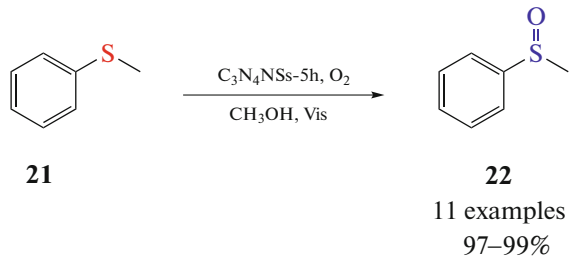

Scheme 11. Selective sulfide oxidation.

2.2. Reduction

In 2016, Nasir et al. reported new strategies for the hydrogenation of alkenes (Scheme 12) using photoreactive catalysts [90]. Fe@g-C_3N_4 was introduced for the hydrogenation of **23** using $NH_2NH_2.H_2O$. Iron nanoparticles had good physical properties like magnetic separability and they were light active, which led to the formation of final products. The combination of the bandgap for 10%Fe@g-C_3N_4 with modification strategies is extremely fortified to find better ways to improve the performance of g-C_3N_4. Light was the only energy source required for this reaction to produce a 99% yield.

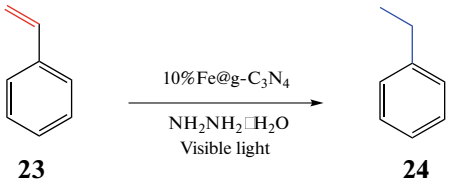

Scheme 12. Hydrogenation of alkenes.

In 2015, authors reported the mpg-C_3N_4/Pd catalyst for the selective addition of hydrogen to nitrobenzene [91]. Scheme 13 shows mpg-C_3N_4/Pd catalyzed hydrogenation of **25** and selectively conversion to **26** within 2 min with water and methanol as solvent. The polymer catalyst produced 96% yield under ambient conditions. The catalysts were easily recoverable and reusability of the catalyst was also checked for several runs.

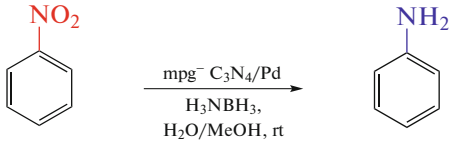

Scheme 13. Hydrogenation of nitroarenes.

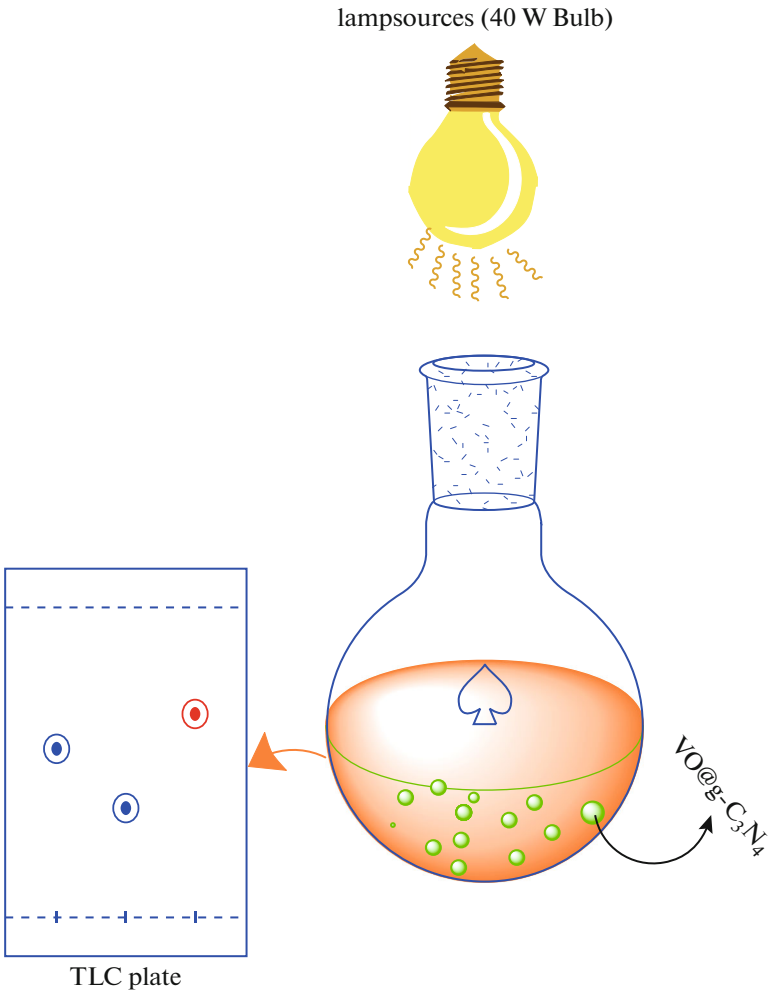

Fig. 3. Schematic reaction condition of arenes.

2.3. Hydroxylation

Verma et al. reported Scheme 14 where the bimetal supported CuAg@g-C_3N_4 system was prepared by the saturated mixture of metal nanoparticles and g-C_3N_4 [92]. Here, Cu and Ag nanoparticles were introduced on the g-C_3N_4 surface. Optimization of the catalyst with 21 trials was done and CuAg@g-C_3N_4 produced 99% yield of **28**. The hydroxylation of **27** was performed under visible light with water and H_2O_2 to generate **28.** The radicals formed on the surface of CuAg@g-C_3N_4 reacted with benzene to form intermediate ions, which reacted with benzene to form phenol.

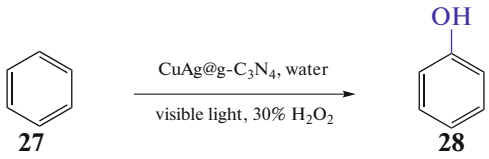

Scheme 14. Hydroxylation of benzene.

2.4. C-H Activation

In 2016, Verma et al. worked on the activation of hydrocarbons shown in Scheme 15 where methyl arenes were involved in C-H activation to oxidize **29** to form **30** [93]. They reported 12 different derivatives of methyl arenes and there was no change in yield with the introduction of the electron-withdrawing or electron-donating group of arene substituent. Graphically, Fig. 3 explains the VO@g-C_3N_4 , which was reactive to activate methylene group and oxygen insertion for the C-H activation reaction. Overall, the surface of g-C_3N_4 was activated by H_2O_2 to create superoxide and hydroxyl radicals in the presence of light. These radicals were more reactive, which attacked the methylene group in the arenes and generated the corresponding aldehydes.

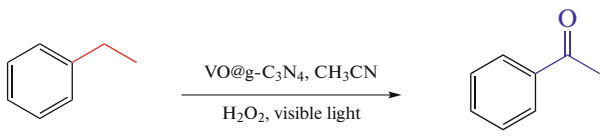

29 **30**
12 examples
85–99%

Scheme 15. C-H activation of hydrocarbons.

2.5. Condensation

Xiang et al. conducted the benzoin synthesis from **31** in the UV region with potassium-supported g-C_3N_4 catalyst for the C-C coupling as shown in Scheme 16 [94]. Here, **31** undergoes C–C coupling through nucleophilic catalysis with the use of cyanide and methyl cyanide as organic solvents in light-mediated conditions. In the last decade, benzoin was synthesized via nucleophilic catalyst, which included cyanide and an organic medium like methyl cyanide, diethyl ether solvents. Benzoin synthesis was done by the green method. Here, water was used as solvent and K-gC_3N_4 acted as a catalyst in the presence of light and 90% yield was obtained. Benzyl alcohol was taken in an oxygenated atmosphere to produce benzaldehyde. Next, the addition of KCN and Xe lamp irradiation to the mixture **32** was obtained in 2 h.

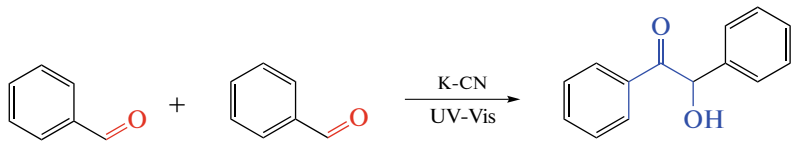

31 **32**

Scheme 16. Benzoin condensation.

2.6. Coupling Reactions

In Scheme 17, Palladium nanoparticles supported by polymeric g-C_3N_4 showed good photocatalytic properties. Many publications on Suzuki coupling reactions have been reported in the last decade. Recently, Li et al. [95] demonstrated a new path to perform the Suzuki coupling reaction. Secondary active radicals reacted with iodobenzene **33a** and boronic acid **33b** to give a high yield of **34.** Here, light energy was used for the C–C bond formation reaction at ambient temperature using a green approach. In recent [96] Au/g-C_3N_4 nanocatalyst was used for stile cross coupling reaction under visible light medium (Scheme 18). To a allyltributylstannane liquid (3 mmol) **35a**, (1-bromoethyl) benzene (1.2 mmol) **35b** and Au/g-C_3N_4 (10 mg), DCM (1 mL) were added. The reaction mixture was irradiated under Xe lamp (300 W) using 420 nm cut-off filter. GC-MS was used to identify the formation of product **36**. The reaction conversion took 10 h to complete the reaction at room temperature. In Scheme 19 [97] exposes the reaction between amines in the presence of cyano-decorated g-C_3N_4 nanosheets (DCNNS). Here the authors describe the difference between DCNNS and g-C_3N_4 nanosheets. Cyano substituted catalyst showed good activity through the preparation of **38** in visible light medium.

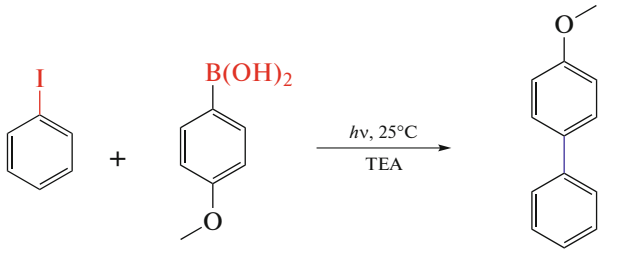

33a **33b** **34**
16 examples,
80–99%

Scheme 17. Suzuki coupling reaction.

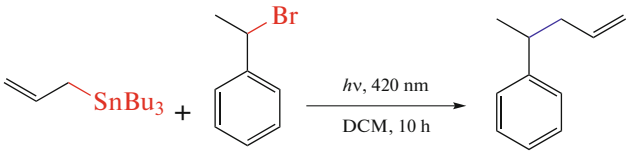

35a **35b** **36**
11 examples,
> 99% selectivity

Scheme 18. Stille coupling reaction.

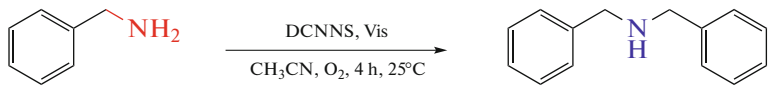

37 **38**
9 examples
96–99%

Scheme 19. Oxidative coupling of amines.

2.7. Other Reactions

Metal-free catalyzed synthesis provides a new platform for organic transformations in the presence of visible light active nanosheets. In 2019, Camussi et al. reported new Diels-Alder and ene reactions with stereochemistry [98]. Oxidized g-C_3N_4 was used to promote chemoselective and unselective oxidation that was related to dienes and alkenes **39** as shown in Scheme 20 and 21.

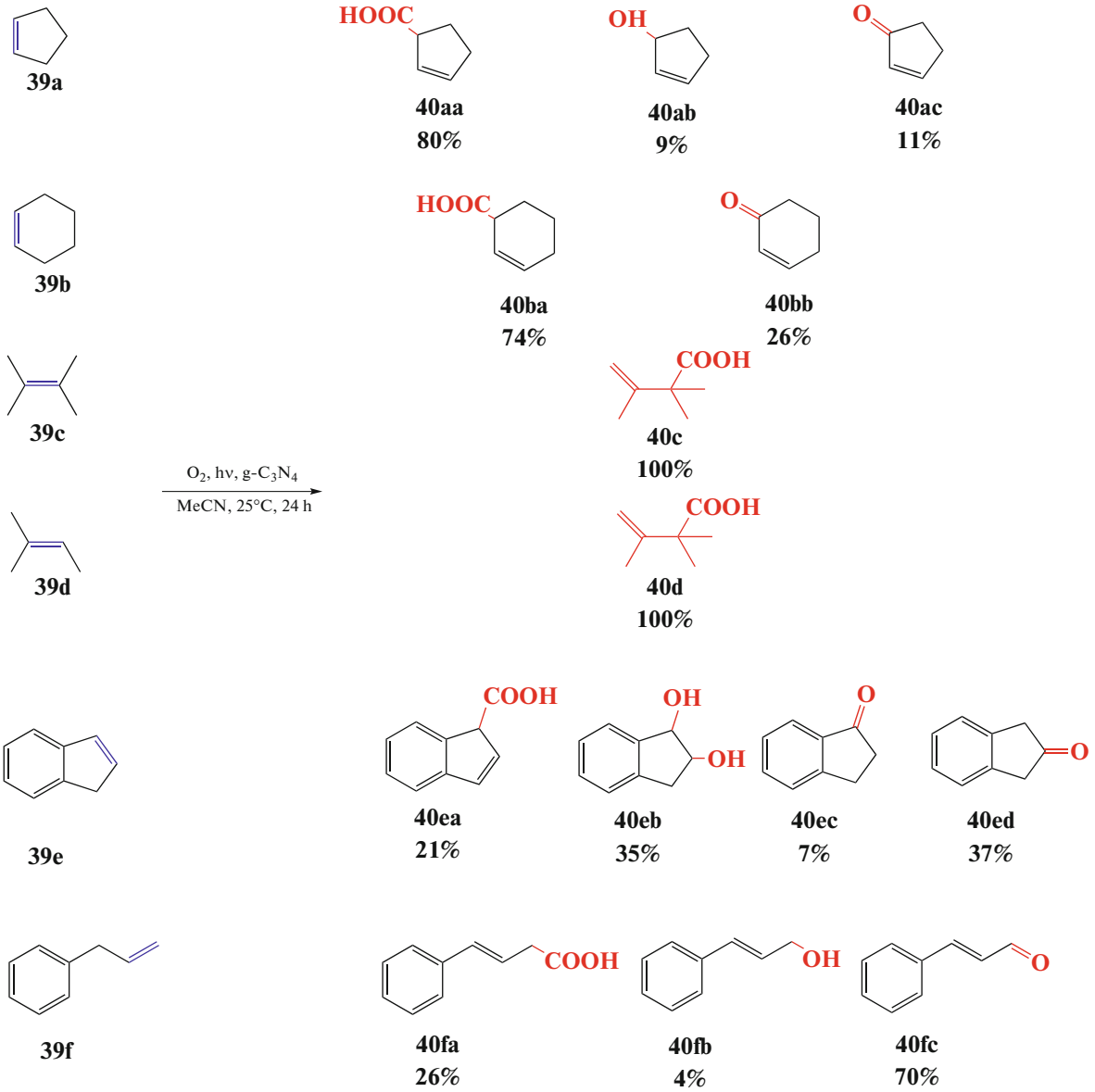

Scheme 20. O_2 and acetonitrile solvent were used for oxidation of reactants to give 100% of selective and unselective products **44**.

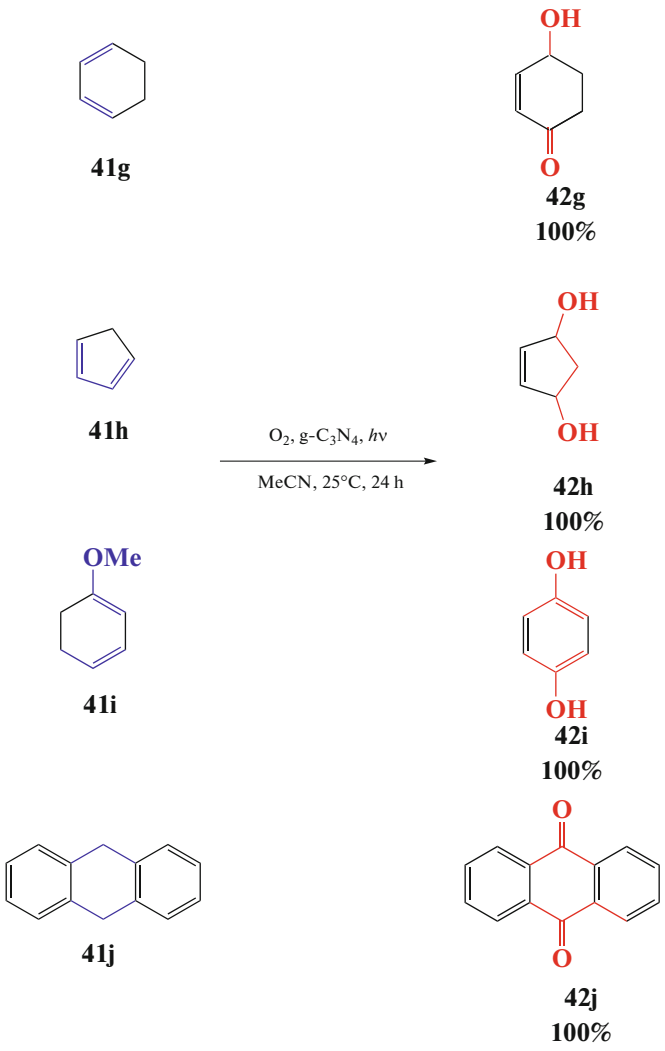

Scheme 21. Ene reactions with singlet Oxygen.

Recently, Allahresani et al. worked on the study of SiO_2 nanoparticles immersed on the surface of g-C_3N_4 (Fig. 4) [99]. Scheme **22** displays one-pot three-component synthesis of **44** with the introduction of SiO_2@g-C_3N_4 nanocomposites using **43a, 43b, 43c** at ambient temperature. A new way has been developed to prepare the spirooxindole **44** with the support of an equal ratio of ethanol and water. The catalyst has many advantages such as easy synthesis, easily recoverable, reusable for more than 5 times and low reaction time with high yield (95%).

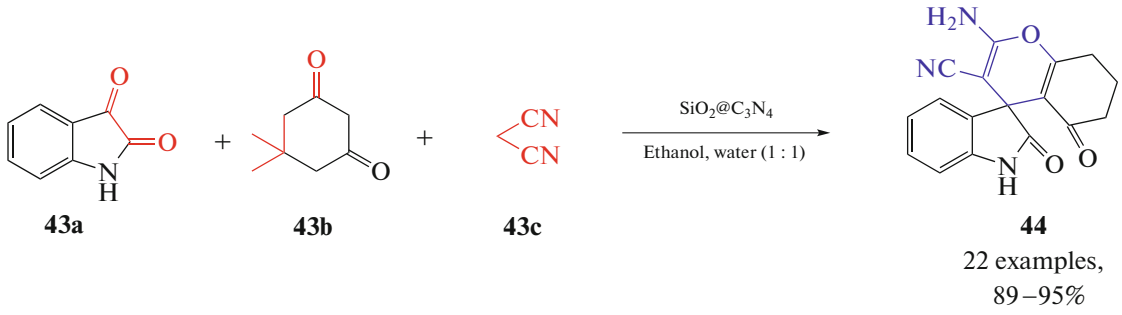

Scheme 22. Green synthesis of spirooxindole.

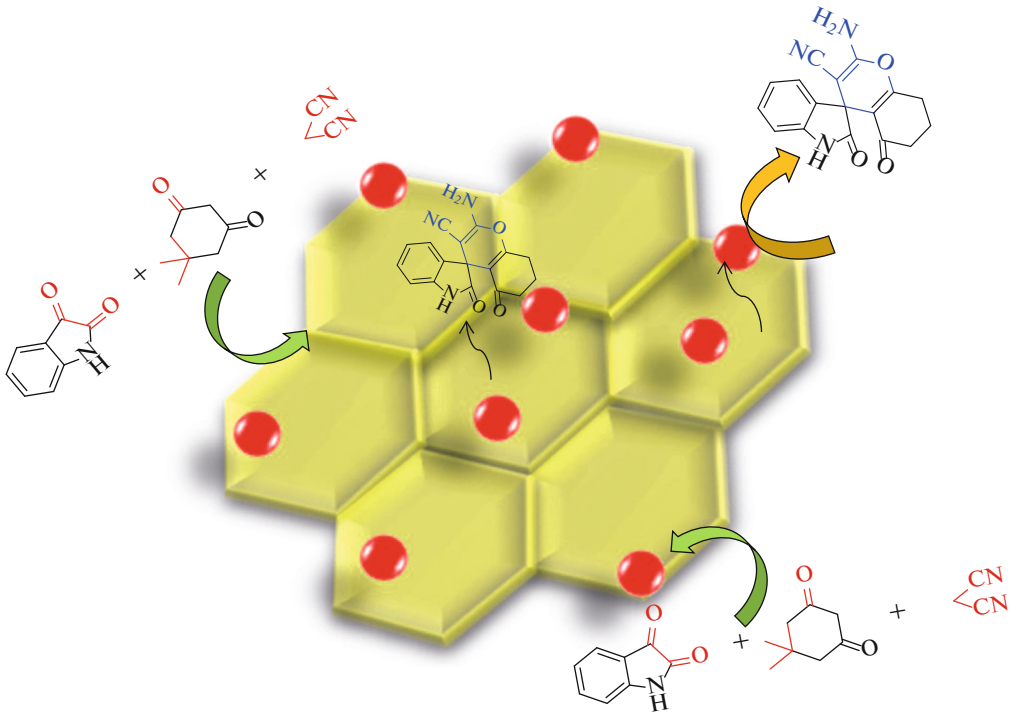

Fig. 4. Formation and reduction mechanism of two dimensional g-C_3N_4 sheet incorporated SiO_2 nanoparticles in spirooxindole organic compounds.

Recently, Verma et al. prepared nanocomposites of Co@g-C_3N_4 to investigate the conversion of various aldehydes **45** to nitriles **46** under visible light irradiation [100]. The interaction between Co and g-C_3N_4 resulted in the tuned bandgap, quenching of photoluminescence (PL), and extended the lifetime of charge carriers for photocatalytic activity. In Scheme **23**, polymer nanocomposites comprising Co@g-C_3N_4 were fabricated as a visible light active photocatalysts. The optimized nanocomposite demonstrated impressive performance and stability with a quantum efficiency and gave 94% yields under visible-light irradiation. The reaction continues for 5 more runs to reuse to get over 90% of conversion. Contrary to the conventional belief one-step four-electron process for photocatalytic organic reaction, this study put forward a new hypothesis of the two-step process; photocatalysis (two-electron) and chemical catalysis (two-electron).

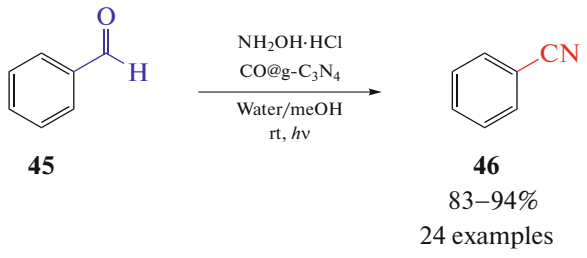

45 **46**
83–94%
24 examples

Scheme 23. Synthesis of nitriles from aldehydes.

Recently Cu/C_3N_4 catalyzed homocoupling of terminal alkynes **47** was reported by Xu et al. [101] in Scheme 24. The reaction was conducted at room temperature in the presence of isopropyl alcohol solvent and KOH base to produce **48**. 14 derivatives and 12 trails were examined to optimize the reaction with maximum yield. The reusability of catalyst showed superior activity for 10 runs. In Scheme 25 [102] simple and efficient visible light-promoted heterogeneous g-C_3N_4-catalyzed switchable divergent synthetic procedure for the synthesis of dihydroquinoxalin-2(1H)-ones and tetrahydroimidazo[1,5-a] quinoxalin-4(5H)-ones using the low-cost and easily available quinoxalin-2(1H)-ones and N-aryl glycines as starting materials. White LED light was used for the irradiation. Here tetrahydroimidazo[1,5-a] quinoxalin-4(5H)-ones were obtained in good yields. This solvent-dependent system has enormous applications like easy operation, short reaction time, high chemoselectivity, a recyclable catalyst, metal-/base-/oxidant-free, and mild reaction conditions. In Scheme 26 [103] Pd supported g-C_3N_4 shows good activity to the preparation of Diethyl (2-(2-hydroxyphenyl) benzopyrano pyrimidinyl phosphonate at ambient conditions. The layers of g-C_3N_4 decorated with Pd^0 prohibit excellent activity towards the formation of **52**. The catalyst shows good activity even after four runs.

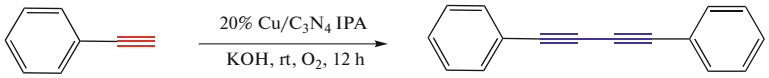

47 **48**
14 examples
52–99%

Scheme 24. Homo-coupling of terminal alkynes.

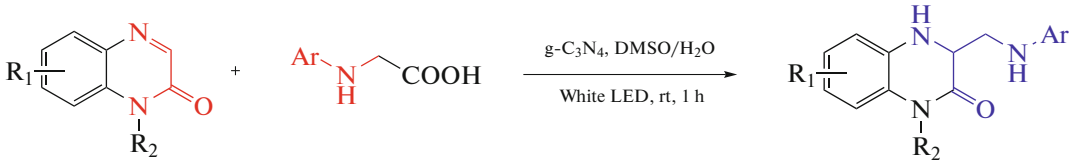

49a **49b** **50**
19 examples
25–89%

Scheme 25. Hydroaminomethylation of Dihydroquinoxalin-2(1H)-ones.

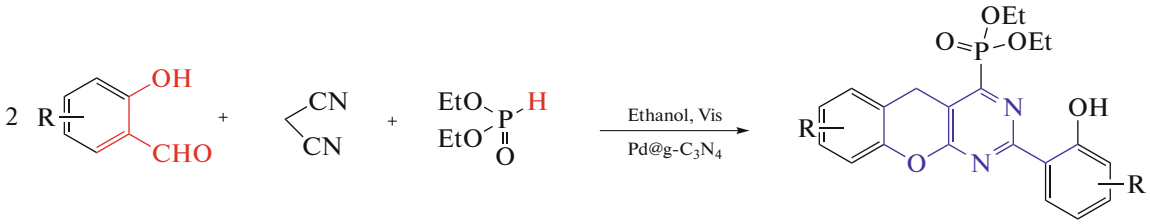

51a **51b** **51c** **52**
10 Examples
91–95%

Scheme 26. Synthesis of Diethyl (2-(2-hydroxyphenyl)benzopy`rano pyrimidinyl phosphonate.

Scheme 27 and 28 were performed in the presence of visible light/ultrasonication in 2021 by Roopan SM [104]. Here the same reaction was worked up within 10mins in visible light medium (Scheme 27). Cu_3-TiO_4/g-C_3N_4 (CNCT) has a bandgap of 2.68 shows good activity in visible light region. Quinoxaline and dihydro-quinazolinone were synthesized with (CNCT) nanocomposites in the presence of visible light/ultrasonication. Here, 12 derivatives of quinoxaline and 11 derivatives of quinazolinone were prepared in a short reaction time. The reusability of the catalyst was also conducted for four cycles.

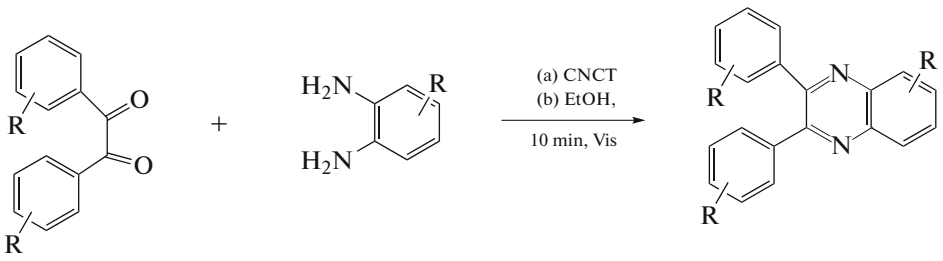

53a **53b** **54**
11 derivatives
80–97%

Scheme 27. Synthesis of quinoxalline.

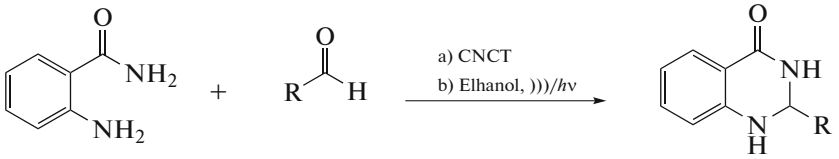

55a **55b** **56**

8 Examples

81–98%

Scheme 28. Synthesis of dihydro- quinazolinone in visible light.

CONCLUSION

The reactions discussed in this review are the preliminary works in g-C_3N_4. We are looking forward to the heterocyclic compounds prepared using the green method using this eco-friendly catalyst. On comparison of the g-C_3N_4 with other traditional catalysts, we found g-C_3N_4 has many advantages like low cost, good physicochemical properties, reusability, visible light active, metal-free catalyst, etc. g-C_3N_4 has proved to be a promising heterogeneous catalyst having good stability for performing heterocyclic reactions. This review will inspire researchers to work on the visible light-mediated synthesis of heterocycles.

ACKNOWLEDGMENTS

We thank the management of the Vellore Institute of Technology for their support and encouragement, especially during COVID-19.

CONFLICT OF INTEREST

All author herewith stating that we don't have any conflict to publish this work.

REFERENCES

1. Patnaik, S., Sahoo, D.P., and Parida, K., An overview on Ag modified g-C_3N_4 based nanostructured materials for energy and environmental applications, *Renew. Sustain. Energy Rev.*, 2018, vol. 82. https://doi.org/10.1016/j.rser.2017.09.026
2. Ren, H.-T., Jia, S.-Y., Wu, Y., et al., Improved photochemical reactivities of Ag_2O/g-C_3N_4 in phenol degradation under UV and visible light, *Ind. Eng. Chem. Res.*, 2014, vol. 53. https://doi.org/10.1021/ie503312x
3. Yang, H., Zhang, S., Cao, R., et al., Constructing the novel ultrafine amorphous iron oxyhydroxide/g-C3N4 nanosheets heterojunctions for highly improved photocatalytic performance, *Sci. Rep.*, 2017, vol. 7. https://doi.org/10.1038/s41598-017-09283-1
4. Chang, F., Zheng, J., Wang, X., et al., Heterojuncted non-metal binary composites silicon carbide/g-C3N4 with enhanced photocatalytic performance, *Mater. Sci. Semicond. Process.*, 2018, vol. 75. https://doi.org/10.1016/j.mssp.2017.11.043
5. Li, X.-H., Chen, J.-S., Wang, X., et al., Metal-free activation of dioxygen by graphene/g-C_3N_4 nanocomposites: Functional dyads for selective oxidation of saturated hydrocarbons, *J. Am. Chem. Soc.*, 2011, vol. 133. https://doi.org/10.1021/ja200997a
6. Babu, S.G. and Karvembu, R., Copper based nanoparticles-catalyzed organic transformations, *Catal. Surv. Asia*, 2013, vol. 17. https://doi.org/10.1007/s10563-013-9159-2
7. Dai, Y., Li, C., Shen, Y., et al., Light-tuned selective photosynthesis of azo- and azoxy-aromatics using graphitic C_3N_4, *Nat. Commun.*, 2018, vol. 9. https://doi.org/10.1038/s41467-017-02527-8
8. Li, F., Xiao, X., Zhao, C., et al., TiO_2-on-g-C_3N_4 double-shell microtubes: In-situ fabricated heterostructures toward enhanced photocatalytic hydrogen evolution, *J. Colloid Interface Sci.,* 2020, vol. 572, p. 22. https://doi.org/10.1016/j.jcis.2020.03.071
9. Tao, R., Li, X., Li, X., et al., TiO_2/$SrTiO_3$/g-C_3N_4 ternary heterojunction nanofibers: gradient energy band, cascade charge transfer, enhanced photocatalytic hydrogen evolution, and nitrogen fixation, *Nanoscale*, 2020, vol. 12. https://doi.org/10.1039/D0NR00219D
10. Liang D, Jing T, Ma Y, et al., Photocatalytic properties of g-C_6N_6/g-C_3N_4 heterostructure: A theoretical study, *J. Phys. Chem. C*, 2016, vol. 120. https://doi.org/10.1021/acs.jpcc.6b08699
11. Kumar, R., Barakat, M.A., and Alseroury, F.A.,. Oxidized g-C_3N_4/polyaniline nanofiber composite for the selective removal of hexavalent chromium, *Sci. Rep.*, 2017, vol 7. https://doi.org/10.1038/s41598-017-12850-1
12. He, Y., Cai, J., Zhang, L., et al., Comparing two new composite photocatalysts, *t*-$LaVO_4$/g-C_3N_4 and *m*-$LaVO_4$/g-C_3N_4, for their structures and performances, *Ind. Eng. Chem. Res.*, 2014, vol. 53. https://doi.org/10.1021/ie4043856
13. Ye, S., Wang, R., Wu, M.-Z., and Yuan, Y.-P., A review on g-C_3N_4 for photocatalytic water splitting and CO_2 reduction, *Appl. Surf. Sci.*, 2015, vol. 358. https://doi.org/10.1016/j.apsusc.2015.08.173
14. Cui, Y., Ding, Z., Liu, P., et al., Metal-free activation of H_2O_2 by g-C_3N_4 under visible light irradiation for the degradation of organic pollutants, *Phys. Chem. Chem.*

Phys., 2012, vol. 14.
https://doi.org/10.1039/C1CP22820J

15. Chen, X., Li, C., Gratzel, M., et al., Nanomaterials for renewable energy production and storage, *Chem. Soc. Rev.*, 2012, vol. 41.
https://doi.org/10.1039/c2cs35230c
16. Goglio, G., Foy, D., and Demazeau, G., State of art and recent trends in bulk carbon nitrides synthesis, *Mater. Sci. Eng. R Rep.*, 2008, vol. 58.
https://doi.org/10.1016/j.mser.2007.10.001
17. Liu, J., An, T., Chen, Z., et al., Carbon nitride nanosheets as visible light photocatalytic initiators and crosslinkers for hydrogels with thermoresponsive turbidity, *J. Mater. Chem. A*, 2017, vol. 5.
https://doi.org/10.1039/C7TA02923C
18. Deng, D., Novoselov, K.S., Fu, Q., et al., Catalysis with two-dimensional materials and their heterostructures, *Nat. Nanotechnol.,* 2016, vol. 11.
https://doi.org/10.1038/nnano.2015.340
19. Jiang, L., Yuan, X., Pan, Y., et al., Doping of graphitic carbon nitride for photocatalysis: A review, *Appl. Catal., B*, 2017, vol. 217.
https://doi.org/10.1016/j.apcatb.2017.06.003
20. Xiong, T., Cen, W., Zhang, Y., and Dong, F., Bridging the g-C_3N_4 interlayers for enhanced photocatalysis, *ACS Catal.,* 2016, vol. 6.
https://doi.org/10.1021/acscatal.5b02922
21. Zhang, W., Jin, H., and Zhang, J., Nb_2CT_xMXene as high-performance energy storage material with Na, K, and liquid K–Na alloy anodes, *Langmuir*, 2021, vol. 37.
https://doi.org/10.1021/acs.langmuir.0c02957
22. Zhang, Q., Deng, J., Xu, Z., et al., High-efficiency broadband C_3N_4 photocatalysts: Synergistic effects from upconversion and plasmons, *ACS Catal.*, 2017, vol. 7.
https://doi.org/10.1021/acscatal.7b02013
23. Zheng, Y., Jiao, Y., Chen, J., et al., Nanoporous graphitic-C_3N_4 carbon metal-free electrocatalysts for highly efficient oxygen reduction, *J. Am. Chem. Soc.*, 2011, vol. 133.
https://doi.org/10.1021/ja209206c
24. Huang, Z., Zeng, X., Li, K., et al., Z-scheme $NiTiO_3$/g-C_3N_4 heterojunctions with enhanced photoelectrochemical and photocatalytic performances under visible LED light irradiation, *ACS Appl. Mater. Interfaces*, 2017, vol. 9:
https://doi.org/10.1021/acsami.7b12386
25. Dong, F., Zhao, Z., Xiong, T., et al., In situ construction of g-C_3N_4/g-C_3N_4 metal-free heterojunction for enhanced visible-light photocatalysis, *ACS Appl. Mater. Interfaces*, 2013, vol. 5.
https://doi.org/10.1021/am403653a
26. Chuang, P.-K., Wu, K.-H., Yeh, T.-F., and Teng, H., Extending the π-conjugation of g-C_3N_4 by incorporating aromatic carbon for photocatalytic H_2 evolution from aqueous solution, *ACS Sustain. Chem. Eng.*, 2016, vol. 4.
https://doi.org/10.1021/acssuschemeng.6b01266
27. Chen, X., Zhang, J., Fu, X., et al., Fe-g-C_3N_4-catalyzed oxidation of benzene to phenol using hydrogen peroxide and visible light, *J. Am. Chem. Soc.*, 2009, vol. 131.
https://doi.org/10.1021/ja903923s
28. Ansari, S.A. and Cho, M.H., Simple and large scale construction of MoS_2-g-C_3N_4 heterostructures using mechanochemistry for high performance electrochemical supercapacitor and visible light photocatalytic applications, *Sci. Rep.*, 2017, vol. 7.
https://doi.org/10.1038/srep43055
29. Cao, S. and Yu, J., g-C_3N_4-based photocatalysts for hydrogen generation, *J. Phys. Chem. Lett.*, 2014, vol. 5.
https://doi.org/10.1021/jz500546b
30. Chen, X., Zhang, L., Zhang, B., et al., Highly selective hydrogenation of furfural to furfuryl alcohol over Pt nanoparticles supported on g-C_3N_4 nanosheets catalysts in water, *Sci. Rep.*, 2016, vol. 6.
https://doi.org/10.1038/srep28558
31. Dai, K., Lu, L., Liu, Q., et al., Sonication assisted preparation of graphene oxide/graphitic-C_3N_4 nanosheet hybrid with reinforced photocurrent for photocatalyst applications, *Dalton Trans.*, 2014, vol. 43.
https://doi.org/10.1039/c3dt53106f
32. Liu, Y.-N., Shen, C.-C., Jiang, N., et al., g-C_3N_4 hydrogen-bonding viologen for significantly enhanced visible-light photocatalytic H_2 evolution, *ACS Catal.*, 2017, vol. 7.
https://doi.org/10.1021/acscatal.7b03266
33. Chen, X., Zhang, J., Fu, X., Antonietti, M., and Wang, X., Fe-g-C_3N_4 catalyzed oxidation of benzene to phenol using hydrogen peroxide and visible light, *J. Am. Chem. Soc.*, 2009, vol. 131, no. 33, p. 11658.
https://doi.org/10.1021/ja903923s
34. He, Y., Cai, J., Li, T., et al., Synthesis, characterization, and activity evaluation of $DyVO_4$/g-C_3N_4 composites under visible-light irradiation, *Ind. Eng. Chem. Res.*, 2012, vol. 51.
https://doi.org/10.1021/ie301774e
35. Bai, X., Wang, L., Zong, R., and Zhu, Y., Photocatalytic activity enhanced via g-C_3N_4 nanoplates to nanorods, *J. Phys. Chem. C*, 2013, vol. 117.
https://doi.org/10.1021/jp402062d
36. Zhang, X., He, S., and Jiang, S.P., WOx/g-C_3N_4 layered heterostructures with controlled crystallinity towards superior photocatalytic degradation and H_2 generation, *Carbon*, 2020, vol. 156.
https://doi.org/10.1016/j.carbo.2019.09.083
37. Gao, Z., Chen, K., Wang, L., et al., Aminated flower-like $ZnIn_2S_4$ coupled with benzoic acid modified g-C_3N_4 nanosheets via covalent bonds for ameliorated photocatalytic hydrogen generation, *Appl. Catal., B*, 2020, vol. 268.
https://doi.org/10.1016/j.apcatb.2019.118462
38. Liu, C., Zhang, Y., Dong, F., et al., Easily and synchronously ameliorating charge separation and band energy level in porous g-C_3N_4 for boosting photooxidation and photoreduction ability, *J. Phys. Chem. C*, 2016, vol. 120.
https://doi.org/10.1021/acs.jpcc.6b01705
39. Wang, X., Maeda, K., Thomas, A., et al., A metal-free polymeric photocatalyst for hydrogen production from water under visible light, *Nat. Mater.*, 2009, vol. 8.
https://doi.org/10.1038/nmat2317
40. Ou, B., Wang, J., Wu, Y., et al., Efficient removal of Cr(VI) by magnetic and recyclable calcined CoFe-

LDH/g-C_3N_4 via the synergy of adsorption and photocatalysis under visible light, *Chem. Eng. J.*, 2020, vol. 380.
https://doi.org/10.1016/j.cej.2019.122600

41. Wang, Y., Sun, J., Li, J., and Zhao, X., Electrospinning preparation of nanostructured g-C_3N_4/$BiVO_4$ composite films with an enhanced photoelectrochemical performance, *Langmuir*, 2017, vol. 33.
https://doi.org/10.1021/acs.langmuir.7b00893
42. Dong, G., Yang, L., Wang, F., et al., Removal of nitric oxide through visible light photocatalysis by g-C_3N_4 modified with perylene imides, *ACS Catal.*, 2016, vol. 6.
https://doi.org/10.1021/acscatal.6b01657
43. Liu, X., Chen, N., Li, Y., et al., A general nonaqueous sol-gel route to g-C_3N_4-coupling photocatalysts: the case of Z-scheme g-C_3N_4/TiO_2 with enhanced photodegradation toward RhB under visible-light, *Sci. Rep.,* 2016, vol. 6.
https://doi.org/10.1038/srep39531
44. Wei, H., McMaster, W.A., Tan, J.Z.Y., et al., Mesoporous TiO_2/g-C_3N_4 microspheres with enhanced visible-light photocatalytic activity, *J. Phys. Chem. C*, 2017, vol. 121.
https://doi.org/10.1021/acs.jpcc.7b06493
45. Tian, S., Zhang, X., and Zhang, Z., Capacitive deionization with MoS_2/g-C_3N_4 electrodes, *Desalination*, 2020, vol. 479.
https://doi.org/10.1016/j.desal.2020.114348
46. Kumar, S., T, S., Kumar, B, et al., Synthesis of magnetically separable and recyclable g-C_3N_4-Fe_3O_4 hybrid nanocomposites with enhanced photocatalytic performance under visible-light irradiation, *J. Phys. Chem. C*, 2013, vol. 117, no. 49, p. 26135.
https://doi.org/10.1021/jp409651g
47. Wang, Q., Wang, P., Xu, P., et al., Visible-light-driven photo-Fenton reactions using Zn1-1.5FeS/g-C_3N_4 photocatalyst: Degradation kinetics and mechanisms analysis, *Appl. Catal., B*, 2020, vol. 266.
https://doi.org/10.1016/j.apcatb.2020.118653
48. Li, K., Gao, S., Wang, Q., et al., In-situ-reduced synthesis of Ti^{3+} self-doped TiO_2/g-C_3N_4 heterojunctions with high photocatalytic performance under LED light irradiation, *ACS Appl. Mater. Interfaces*, 2015, vol. 7.
https://doi.org/10.1021/am508505n
49. Li, X.-H., Wang, X., and Antonietti, M., Solvent-free and metal-free oxidation of toluene using O_2 and g-C_3N_4 with nanopores: Nanostructure boosts the catalytic selectivity, *ACS Catal.*, 2012, vol. 2.
https://doi.org/10.1021/cs300413x
50. Yan, S.C., Li, Z.S., and Zou, Z.G., Photodegradation performance of g-C_3N_4 fabricated by directly heating melamine, *Langmuir*, 2009, vol. 25.
https://doi.org/10.1021/la900923z
51. Pawar, R.C., Kang, S., Park, J.H.,, et al., Room-temperature synthesis of nanoporous 1D microrods of graphitic carbon nitride (g-C_3N_4) with highly enhanced photocatalytic activity and stability, *Sci. Rep.*, 2016, vol. 6.
https://doi.org/10.1038/srep31147
52. Samanta, S., Khilari, S., Pradhan, D., and Srivastava, R., An efficient, visible light driven, selective oxidation of aromatic alcohols and amines with O_2 using $BiVO_4$/g-C_3N_4 nanocomposite: A systematic and comprehensive study toward the development of a photocatalytic process, *ACS Sustain. Chem. Eng.*, 2017, vol. 5.
https://doi.org/10.1021/acssuschemeng.6b02902
53. Shi, W., Li, M., Huang, X., et al., Facile synthesis of 2D/2D $Co_3(PO_4)_2$/g-C_3N_4 heterojunction for highly photocatalytic overall water splitting under visible light, *Chem. Eng. J.*, 2020, vol. 382.
https://doi.org/10.1016/j.cej.2019.122960
54. Palaniraja, J. and Roopan, S.M., UV-light induced domino type reactions: synthesis and photophysical properties of unreported nitrogen ring junction quinazolines, *RSC Adv.*, 2015, vol. 5.
https://doi.org/10.1039/C5RA00229J
55. Bavykina, A., Kolobov, N., Khan, I.S., et al., Metal–organic frameworks in heterogeneous catalysis: Recent progress, new trends, and future perspectives, *Chem. Rev.*, 2020, vol. 120.
https://doi.org/10.1021/acs.chemrev.9b00685
56. Hemalatha, K. and Madhumitha, G., Inhibition of poly(adenosine diphosphate-ribose)polymerase using quinazolinone nucleus, *Appl. Microbiol. Biotechnol.*, 2016, vol. 100.
https://doi.org/10.1007/s00253-016-7731-1
57. Shi, H., Chen, G., Zhang, C., and Zou, Z., Polymeric g-C_3N_4 coupled with $NaNbO_3$ nanowires toward enhanced photocatalytic reduction of CO_2 into renewable fuel, *ACS Catal.*, 2014, vol. 4.
https://doi.org/10.1021/cs500848f
58. Xie, Q., He, W., Liu, S., et al., Bifunctional S-scheme g-C_3N_4/Bi/$BiVO_4$ hybrid photocatalysts toward artificial carbon cycling, *Chin. J. Catal.*, 2020, vol. 41 (19, vol. 63481-9
https://doi.org/10.1016/S1872-2067
59. Wang, X., Yang, W., Li, F., et al., In situ microwave-assisted synthesis of porous N-TiO_2/g-C_3N_4 heterojunctions with enhanced visible-light photocatalytic properties, *Ind. Eng. Chem. Res.*, 2013, vol. 52.
https://doi.org/10.1021/ie402820v
60. Wang, K., Li, Y., Li, J., and Zhang, G., Boosting interfacial charge separation of $Ba_5Nb_4O_{15}$/g-C_3N_4 photocatalysts by 2D/2D nanojunction towards efficient visible-light driven H_2 generation, *Appl. Catal., B*, 2020, vol. 263.
https://doi.org/10.1016/j.apcatb.2019.05.032
61. Xiang, Q., Yu, J., and Jaroniec, M., Preparation and enhanced visible-light photocatalytic H_2-production activity of graphene/C_3N_4 composites, *J. Phys. Chem. C*, 2011, vol. 115.
https://doi.org/10.1021/jp200953k
62. Zhang, L., Hao, X., Li, Y., and Jin, Z., Performance of WO_3/g-C_3N_4 heterojunction composite boosting with NiS for photocatalytic hydrogen evolution, *Appl. Surf. Sci.*, 2020, vol. 499.
https://doi.org/10.1016/j.apsusc.2019.143862
63. Wang, T., Nie, C., Ao, Z., et al., Recent progress in g-C_3N_4 quantum dots: Synthesis, properties and applications in photocatalytic degradation of organic pollutants. *J. Mater. Chem. A*, 2020, vol. 8.
https://doi.org/10.1039/C9TA11368A

64. Zhang, J., Zhang, M., Zhang, G., and Wang, X., Synthesis of carbon nitride semiconductors in sulfur flux for water photoredox catalysis, *ACS Catal.*, 2012, vol. 2. https://doi.org/10.1021/cs300167b

65. Kaya, K., Kiskan, B., Kumru, B., et al., An oxygen-tolerant visible light induced free radical polymerization using mesoporous graphitic carbon nitride, *Eur. Polym. J.*, 2020, vol. 122. https://doi.org/10.1016/j.eurpolymj.2019.109410

66. Xia, Y., Fang, R., Xiao, Z., et al., Confining sulfur in N-doped porous carbon microspheres derived from microalgaes for advanced lithium-sulfur batteries, *ACS Appl. Mater. Interfaces*, 2017, vol. 9. https://doi.org/10.1021/acsami.7b05798

67. Zhang, Y., Pan, Q., Chai, G., et al., Synthesis and luminescence mechanism of multicolor-emitting g-C_3N_4 nanopowders by low temperature thermal condensation of melamine, *Sci. Rep.*, 2013, vol. 3. https://doi.org/10.1038/srep01943

68. Adeleke, J.T., Theivasanthi, T., Thiruppathi, M., et al., Photocatalytic degradation of methylene blue by ZnO/$NiFe_2O_4$ nanoparticles, *Appl. Surf. Sci.*, 2018, vol. 455. https://doi.org/10.1016/j.apsusc.2018.05.184

69. Zhou, M., Wang, S., Yang, P., et al., Boron carbon nitride semiconductors decorated with CdS nanoparticles for photocatalytic reduction of CO_2, *ACS Catal.*, 2018, vol. 8. https://doi.org/10.1021/acscatal.8b00104

70. Gao, M., Feng, J., He, F., et al., Carbon microspheres work as an electron bridge for degrading high concentration MB in $CoFe_2O_4$ carbon microsphere/g-C_3N_4 with a hierarchical sandwich-structure, *Appl. Surf. Sci.*, 2020, vol. 507. https://doi.org/10.1016/j.apsusc.2019.145167

71. Wu, X., Wang, X., Wang. F., and Yu, H., Soluble g-C_3N_4 nanosheets: Facile synthesis and application in photocatalytic hydrogen evolution, *Appl. Catal., B*, 2019, vol. 247. https://doi.org/10.1016/j.apcatb.2019.01.088

72. Qamar, M.A., Shahid, S., and Javed, M., Synthesis of dynamic g-C_3N_4/FeZnO nanocomposites for environmental remediation applications, *Ceram. Int.*, 2020, vol. 46. https://doi.org/10.1016/j.ceramint.2020.05.294

73. Yuan, Y.-J., Shen, Z., Wu, S., et al., Liquid exfoliation of g-C_3N_4 nanosheets to construct 2D-2D MoS_2/g-C_3N_4 photocatalyst for enhanced photocatalytic H_2 production activity, *Appl. Catal., B*, 2019, vol. 246. https://doi.org/10.1016/j.apcatb.2019.01.043

74. Savateev, A. and Antonietti, M., Ionic carbon nitrides in solar hydrogen production and organic synthesis: exciting chemistry and economic advantages, *ChemCatChem*, 2019, vol. 11. https://doi.org/10.1002/cctc.201901076

75. Yang, Q., Pan, G., Wei, J., et al., Remarkable activity of potassium-modified carbon nitride for heterogeneous photocatalytic decarboxylative alkyl/acyl radical addition and reductive dimerization of *para*-quinone methides, *ACS Sustain. Chem. Eng.*, 2021, vol. 9. https://doi.org/10.1021/acssuschemeng.0c08771

76. Akhundi, A., Badiei, A., Ziarani, G.M., et al., Graphitic carbon nitride-based photocatalysts: Toward efficient organic transformation for value-added chemicals production, *Mol. Catal.* 2020, vol. 488. https://doi.org/10.1016/j.mcat.2020.110902

77. Yang, Q., Pan, G., Wei, J., et al., Remarkable activity of potassium-modified carbon nitride for heterogeneous photocatalytic decarboxylative alkyl/acyl radical addition and reductive dimerization of *para*-quinone methides, *ACS Sustain. Chem. Eng.*, 2021, vol. 9. https://doi.org/10.1021/acssuschemeng.0c08771

78. Li, X.-H., Wang, X., and Antonietti, M., Solvent-free and metal-free oxidation of toluene using O_2 and g-C_3N_4 with nanopores: Nanostructure boosts the catalytic selectivity, *ACS Catal.*, 2012, vol. 2. https://doi.org/10.1021/cs300413x

79. Rai, V.K., Verma, F., Mahata, S., et al., Metal doped-C_3N_4/Fe_2O_4: Efficient and versatile heterogenous catalysts for organic transformations, *Curr. Org. Chem.*, 2019, vol. 23. https://doi.org/10.2174/1385272823666190709113758

80. Su, F., Mathew, S.C., Lipner, G., et al., mpg-C_3N_4-catalyzed selective oxidation of alcohols using O_2 and visible light, *J. Am. Chem. Soc.*, 2010, vol. 132. https://doi.org/10.1021/ja102866p

81. Shvalagin, V.V., Kompanets, M.O., Kutsenko, O.S., Kuchmy, S.Ya., and Skoryk, M.A., Remarkable activity of potassium-modified carbon nitride for heterogeneous photocatalytic decarboxylative alkyl/acyl radical addition and reductive dimerization of *para*-quinone methides, *Theor. Exp. Chem.*, 2020, vol. 56, p. 111. https://doi.org/10.1021/acssuschemeng.0c08771

82. Li, X.-H., Chen, J.-S., Wang, X., et al., Metal-free activation of dioxygen by graphene/g-C_3N_4 nanocomposites: Functional dyads for selective oxidation of saturated hydrocarbons, *J. Am. Chem. Soc.*, 2011, vol. 133. https://doi.org/10.1021/ja200997a

83. Marci, G., Garcia-Lopez, E.I., and Palmisano, L., Polymeric carbon nitride (C_3N_4) as heterogeneous photocatalyst for selective oxidation of alcohols to aldehydes, *Catal. Today*, 2018, vol. 315. https://doi.org/10.1016/j.cattod.2018.03.038

84. Verma, S., Photocatalytic oxidation of aromatic amines using MnO_2@G-C_3N_4, *Adv. Mater. Lett.*, 2017, vol. 8. https://doi.org/10.5185/amlett.2017.1453

85. Mohlmann, L., Ludwig, S., and Blechert, S., NHC-catalysed highly selective aerobic oxidation of nonactivated aldehydes, *Beilstein J. Org. Chem.*, 2013, vol. 9. https://doi.org/10.3762/bjoc.9.65

86. Xu, H., Wu, K., Tian, J., et al., Recyclable Cu/C_3N_4 composite catalysed homo- and cross-coupling of terminal alkynes under mild conditions, *Green Chem.*, 2018, vol. 20. https://doi.org/10.1039/C7GC03120C

87. Xu, S., Zhou, P., Zhang, Z., et al., Selective oxidation of 5-hydroxymethylfurfural to 2,5-furandicarboxylic acid using O_2 and a photocatalyst of Co-thioporphyrazine bonded to g-C_3N_4, *J. Am. Chem. Soc.*, 2017, vol. 139. https://doi.org/10.1021/jacs.7b08861

88. Yu, C., Xie, X., and Zhang, N., Selectivity control of organic chemical synthesis over plasmonic metal-based

photocatalysts, *Catal. Sci. Technol.*, 2021, vol. 11. https://doi.org/10.1039/D0CY02030C

89. Li, J., Chen, Y., Yang, X., et al., Visible-light-mediated high-efficiency catalytic oxidation of sulfides using wrinkled C_3N_4 nanosheets, *J. Catal.,* 2020, vol. 381. https://doi.org/10.1016/j.jcat.2019.11.041
90. Baig, R.B.N., Verma, S., Varma, R.S., and Nadagouda, M.N., Magnetic Fe@g-C_3N_4: A photoactive catalyst for the hydrogenation of alkenes and alkynes, *ACS Sustain. Chem. Eng.*, 2016, vol. 4. https://doi.org/10.1021/acssuschemeng.5b01610
91. Fageria, P., Uppala, S., Nazir, R., et al., Synthesis of monometallic (Au and Pd) and bimetallic (AuPd) nanoparticles using carbon nitride (C_3N_4) quantum dots via the photochemical route for nitrophenol reduction, *Langmuir*, 2016, vol. 32. https://doi.org/10.1021/acs.langmuir.6b02375
92. Gong, Y., Zhang, P., Xu, X., et al., A novel catalyst Pd@ompg-C_3N_4 for highly chemoselective hydrogenation of quinoline under mild conditions, *J. Catal.*, 2013, vol. 297. https://doi.org/10.1016/j.jcat.2012.10.018
93. Wang, W., Wei, Y., Jiang, X., et al., Rational designed polymer as a metal-free catalyst for hydroxylation of benzene to phenol with dioxygen, *Catal. Lett.*, 2021, vol. 151. https://doi.org/10.1007/s10562-020-03392-9
94. Sun, X. Jiang, D., Zhang, L., and Wang, W., Alkaline modified g-C_3N_4 photocatalyst for high selective oxide coupling of benzyl alcohol to benzoin, *Appl. Catal., B*, 2018, vol. 220. https://doi.org/10.1016/j.apcatb.2017.08.057
95. Azizi, N. and Farhadi, E., Synthesis of magnetically separable and recyclable g-C_3N_4–Fe_3O_4 hybrid nanocomposites with enhanced photocatalytic performance under visible-light irradiation, *J. Phys. Chem. C*, 2013, vol. 117. https://doi.org/10.1021/jp409651g
96. Yu, Q., Lin, X., Li, X., and Chen, J., Room-temperature synthesis of nanoporous 1D microrods of graphitic carbon nitride (g-C3N4) with highly enhanced photocatalytic activity and stability, *Chem. Res. Chin. Univ.*, 2020, vol. 13, p. 162.
97. Zhang, D., Han, X., Dong, T., et al., Promoting effect of cyano groups attached on g-C_3N_4 nanosheets towards molecular oxygen activation for visible light-driven aerobic coupling of amines to imines, *J. Catal.*, 2018, vol. 366. https://doi.org/10.1016/j.jcat.2018.08.018
98. Camussi, I., Mannucci, B., Speltini, A., et al., g-C_3N_4-singlet oxygen made easy for organic synthesis: Scope and limitations, *ACS Sustain. Chem. Eng.*, 2019, vol. 7. https://doi.org/10.1021/acssuschemeng.8b06164
99. Allahresani, A., Taheri, B., and Nasseri, M.A., Synthesis of magnetically separable and recyclable g-C3N4–Fe3O4 hybrid nanocomposites with enhanced photocatalytic performance under visible-light irradiation, *Res. Chem. Intermed.*, 2018, vol. 4, p. 1173. https://doi.org/10.1021/ja903923s
100. Verma, F., Shukla, P., Bhardiya, S.R., Singh, M., Rai, A., and Rai, V.K., Electrospinning preparation of nanostructured g-C3N4/BiVO4 composite films with an enhanced photoelectrochemical performance, *Catal. Commun.*, 2019, vol. 119, p. 76. https://doi.org/10.1021/jp402062d
101. Rai, V.K., Verma, F., Mahata, S., et al., Metal doped-C_3N_4/Fe_2O_4: Efficient and versatile heterogenous catalysts for organic transformations, *Curr. Org. Chem.*, 2019, vol. 23. https://doi.org/10.2174/1385272823666190709113758
102. Zeng, F.-L,, Chen, X.-L., Sun, K., et al., Visible-light-induced metal-free cascade cyclization of *N*-arylpropiolamides to 3-phosphorylated, trifluoromethylated and thiocyanated azaspiro[4.5]trienones, *Org. Chem. Front.*, 2021, vol. 8. https://doi.org/10.1039/D0QO01410A
103. Santhisudha, S., Mohan, G., Rani, T.S., Reddy, P.V.G., and Reddy, C.S., Nanoporous graphitic-C_3N_4@carbon metal-free electrocatalysts for highly efficient oxygen reduction, *Lett. Drug Des. Discov.*, 2019, vol. 16, p. 721. https://doi.org/10.1021/ja200997b
104. Arunachalapandi, M. and Roopan, S.M., Ultrasound/visible light-mediated synthesis of N-heterocycles using g-C_3N_4/Cu_3TiO_4 as sonophotocatalyst, *Res. Chem. Intermed.,* 2021, vol. 47. https://doi.org/10.1007/s11164-021-04461-316